Green's function approach to the magnetic properties of the kagomé antiferromagnet

B. H. Bernhard*
Dep. de Física, Universidade do Estado de Santa Catarina, C.P. 631, 89223-100 Joinville, SC, Brazil

B. Canals† and C. Lacroix‡
Laboratoire de Magnétisme Louis Néel, CNRS, B.P. 166, 38042 Grenoble Cedex9, France

(Dated: February 1, 2008)

The $S = 1/2$ Heisenberg antiferromagnet is studied on the kagomé lattice by using a Green's function method based on an appropriate decoupling of the equations of motion. Thermodynamic properties as well as spin-spin correlation functions are obtained and characterize this system as a two-dimensional quantum spin liquid. Spin-spin correlation functions decay exponentially with distance down to low temperature and the calculated missing entropy at $T = 0$ is found to be $0.46 \ln 2$. Within the present scheme, the specific heat exhibits a single peak structure and a T^2 dependence at low temperature.

PACS numbers: 75.10.Jm,75.40.-s,75.50.Ee

I. INTRODUCTION

Antiferromagnetic spin systems on fully frustrated lattices show many unusual behaviors in magnetic and thermal properties[1,2]. One of the main ingredients is that their unit cell allows for a continuous degree of freedom and that the connectivity (corner sharing) allows for an extensive number of these degrees of freedom in the classical ground state. More subtle phenomena appear when looking at quantum models on these lattices as quantum fluctuations may induce very unsusual ground states. In particular, wether the quantum ground state on fully frustrated lattices may not break the lattice symmetry nor the spin group symmetry is still a highly debated question. A lot of work has been done to answer this question in the framework of the proposition of Anderson[3], looking first at Resonating Valence Bond states.

One of the most studied candidates is the quantum S=1/2 Heisenberg antiferromagnet on the kagomé lattice. Using various methods[4,5,6,7,8,9,10,11,12], it has been shown that the low temperature physics should be dominated by short range RVB states which produce a continuum of singlet states between the $S = 0$ ground state and the first excited $S = 1$ state. A still controversial question is the presence of a very low temperature peak in the specific heat, much below the one corresponding to the onset of short range correlations, that could be ascribed to a high density of singlet states in the singlet-triplet spin gap. Associated to this low temperature peak is the missing (or not) entropy that would characterize an ordered or a disordered ground state.

The experimental relevance of the model is extremely fragile as, in real compounds, many other parameters may drive the physics to very different universality classes, described through inclusion of next nearest neighbor interactions[13], disorder[14], antisymmetric interactions[15], etc... Nevertheless, in many cases, the Heisenberg antiferromagnet is a good starting point as it is generally believed that many properties of realistic systems come from deviations from the Heisenberg limit. Examples are the layered oxide $SrCr_{9p}Ga_{12-9p}O_{19}$[16,17,18] ($S = 3/2$) or the organic pseudo-$S = 1$ compound m-MPYNN.BF_4[19].

In this paper, the properties of the Heisenberg S=1/2 kagomé antiferromagnet are addressed by using a spin Green's functions technique. One of the advantages of the method is that it is well suited for magnetic systems with no long range order as it uses a decoupling scheme based on short ranged spin correlations. This method was previously introduced by Kondo and Yamagi[20] in the context of the one-dimensional Heisenberg model as a theory of spin-waves in absence of long-range order. More recently, it has been used to address different problems[21,22] and can be extended to include magnetic phases[23]. Here, the formalism is used to compute thermodynamic and magnetic quantities at all temperatures, like the internal energy, specific heat, entropy, magnetic susceptibility and structure factor. Correlation functions are also computed at all temperatures and for various separation distances. In the next section, the approximation is presented and results are discussed in Sec. III.

II. MODEL AND APPROXIMATION

The antiferromagnetic Heisenberg model is defined by the Hamiltonian

$$\mathcal{H} = \frac{1}{2} \sum_{ij} J_{ij} \ \mathbf{S}_i \cdot \mathbf{S}_j. \tag{1}$$

where we assume $S = 1/2$ and a nearest-neighbor exchange

$$J_{ij} = \begin{cases} J(>0) & \text{if } i,j \text{ are nearest neighbors} \\ 0 & \text{otherwise.} \end{cases} \tag{2}$$

The spin susceptibility

$$\chi_{ij}(\omega) \equiv \ll S_i^-; S_j^+ \gg_\omega \tag{3}$$

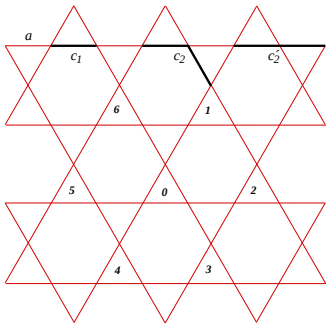

FIG. 1: The kagomé lattice.

is obtained by a Fourier transformed Green's function

$$\ll A; B \gg_\omega = \int \ll A; B \gg_t e^{i\omega t} dt \tag{4}$$

where

$$\ll A; B \gg_t \equiv -i\theta(t) \left\langle \left[\hat{A}(t), \hat{B}(0) \right] \right\rangle . \tag{5}$$

¿From the equation of motion of the operator $\hat{A}(t)$ in the Heisenberg representation, the Green's functions above must satisfy the equation

$$\omega \ll A; B \gg_\omega = \langle [A, B] \rangle + \ll [A, \mathcal{H}]; B \gg_\omega . \tag{6}$$

The spin susceptibility of the present model can be obtained by

$$\omega \chi_{ij}(\omega) = -2\delta_{ij} \langle S_i^z \rangle + \sum_k J_{ik} \left(\Gamma_{kij}(\omega) - \Gamma_{ikj}(\omega) \right) . \tag{7}$$

The three operator Green's functions

$$\Gamma_{ikj}(\omega) \equiv \ll S_i^z S_k^-; S_j^+ \gg_\omega \tag{8}$$

must also obey their corresponding equations

$$\begin{aligned} \omega \Gamma_{ikj}(\omega) = & \left(\delta_{ij} - \delta_{kj}\right) \left\langle S_i^+ S_k^- \right\rangle_\omega \\ & + 1/2 \sum_l J_{il} \ll \left(S_i^+ S_l^- - S_i^- S_l^+ \right) S_k^-; S_j^+ \gg_\omega \\ & + \sum_l J_{kl} \ll S_i^z \left(S_l^z S_k^- - S_k^z S_l^- \right); S_j^+ \gg, \end{aligned} \tag{9}$$

As higher-order Green's functions are generated, one obtains an infinite hierarchy of equations which have to be decoupled in order to obtain $\chi_{ij}(\omega)$.

In a frustrated lattice, one is constrained to the non-magnetic phase, where $\langle S_i^z \rangle = \langle S_i^\pm \rangle = 0$ and $\langle S_i^+ S_j^- \rangle = 2 \langle S_i^z S_j^z \rangle$.

Here we adopt an extension of the Kondo-Yamaji decoupling approximation for the kagomé lattice, assuming (only for different sites i, l, k)

$$\begin{aligned} \ll S_i^- S_l^+ S_k^-; S_j^+ \gg_\omega \; \approx \; & \alpha \left\langle S_i^- S_l^+ \right\rangle \chi_{kj}(\omega) \\ & + \alpha \left\langle S_l^+ S_k^- \right\rangle \chi_{ij}(\omega), \end{aligned} \tag{10}$$

$$\ll S_i^z S_l^z S_k^-; S_j^+ \gg_\omega \; \approx \; \alpha \left\langle S_i^z S_l^z \right\rangle \chi_{kj}(\omega). \tag{11}$$

The static correlation functions $\langle S_i^+ S_j^- \rangle$ between spins at the lattice positions $\mathbf{R}_i$ and $\mathbf{R}_j$ depend on the distance $d = |\mathbf{R}_i - \mathbf{R}_j|$, on the number n of bonds between sites i and j, and on the lattice symmetry. As a shorthand notation, we shall call the local correlation as $c_0 = \langle S_i^+ S_i^- \rangle$, the nearest-neighbor correlation as c_1 and the next-nearest-neighbor correlations as c_2 and c_2' (the former corresponding to the shortest distance, as illustrated in figure 1). We also introduce $\tilde{c}_n^{(\prime)} = \alpha c_n^{(\prime)}$. The parameter α is useful to enforce the condition $c_0 = 1/2$[20].

These correlation functions can be evaluated from the spin susceptibility as

$$\langle S_j^+ S_i^- \rangle = -\frac{1}{\pi} \int \frac{\mathrm{Im}\chi_{ij}(\omega + i\eta)}{1 - e^{-\beta\omega}} \, d\omega. \tag{12}$$

Thus, c_1, c_2, and c_2' and also the parameter α appearing in Eqs. 10-11 must be evaluated selfconsistently.

Applying approximation 10-11 to the kagomé lattice yields

$$\begin{aligned} & \left[\omega^2 - 4J^2\tilde{c}\right] \chi_{ij}(\omega) = -8Jc_1\delta_{ij} + 2c_1 J_{ij} \\ & + J\tilde{c}_1 \sum_k J'_{ik}\chi_{kj}(\omega) - J\left(\tilde{c} + 2\tilde{c}_1\right) \sum_k J_{ik}\chi_{kj}(\omega), \end{aligned} \tag{13}$$

where

$$\tilde{c} = 1/2 + \tilde{c}_1 + \tilde{c}_2 + \tilde{c}_2' \tag{14}$$

and

$$J'_{ij} = \begin{cases} J & \text{if i, j are next-nearest neighbors,} \\ 0 & \text{otherwise.} \end{cases} \tag{15}$$

By working directly with the $\tilde{c}_n^{(\prime)}$, the numerical problem is reduced to only two selfconsistent parameters, $\tilde{c}_1$ and $\tilde{c}_2 + \tilde{c}_2'$, from which one can obtain $\alpha = 2\tilde{c}_0$.

With reference to the underlying triangular lattice, the approximate equation 13 can be rewritten in matrix form

$$\begin{aligned} & \left[\omega^2 - 4J^2\tilde{c}\right] \boldsymbol{\chi}_{ij}(\omega) = -2c_1 \left(4J\delta_{ij}\boldsymbol{1} - \boldsymbol{J}_{ij}\right) \\ & + J\tilde{c}_1 \sum_k \boldsymbol{J}'_{ik}\boldsymbol{\chi}_{kj}(\omega) - J\left(\tilde{c} + 2\tilde{c}_1\right) \sum_k \boldsymbol{J}_{ik}\boldsymbol{\chi}_{kj}(\omega) \, , \end{aligned} \tag{16}$$

where $\boldsymbol{J}_{ij}$ and $\boldsymbol{J}'_{ij}$ are the exchange matrices connecting neighboring triangles. As indicated in Fig. 1, each triangle is surrounded by six neighboring triangles, all of them contributing to both types of exchange matrices.

The elements of the dynamic susceptibility matrix are defined as

$$\chi^{ab}(\mathbf{q},\omega) = \frac{1}{N}\sum_{i,j}\chi^{ab}_{ij}(\omega)\; e^{-i\mathbf{q}\cdot(\mathbf{R}^a_i-\mathbf{R}^b_j)} \tag{17}$$

where $\mathbf{R}^a_i = \mathbf{R}_i + \mathbf{T}_a$, $\mathbf{R}_i$ is the lattice position of the i-th triangle, and the vectors $\mathbf{T}_a$ indicate the position of site a in the triangular unit cell ($a = 1, 2, 3$).

Applying a corresponding Fourier transformation to equation 16 gives

$$\boldsymbol{\chi}(\mathbf{q},\omega) = -2c_1\boldsymbol{A}^{-1}(\mathbf{q},\omega)\;\boldsymbol{B}(\mathbf{q}) \tag{18}$$

where

$$\begin{aligned}\boldsymbol{A}(\mathbf{q},\omega) &= \left(\omega^2 - 4J^2\tilde{c}\right)\boldsymbol{1} - J\tilde{c}_1\boldsymbol{J}'(\mathbf{q}) \\ &\quad + J\left(\tilde{c}+2\tilde{c}_1\right)\boldsymbol{J}(\mathbf{q}), \qquad (19)\\ \boldsymbol{B}(\mathbf{q}) &= 4J\boldsymbol{1} - \boldsymbol{J}(\mathbf{q}), \qquad (20)\end{aligned}$$

where $\boldsymbol{J}(\mathbf{q})$ and $\boldsymbol{J}'(\mathbf{q})$ are the Fourier transform of the exchange matrices $\boldsymbol{J}_{ij}$ and $\boldsymbol{J}'_{ij}$,

$$\boldsymbol{J}(\mathbf{q}) = 2J\begin{pmatrix} 0 & \cos[(x-\sqrt{3}y)/4] & \cos[(x+\sqrt{3}y)/4] \\ \cos[(x-\sqrt{3}y)/4] & 0 & \cos(x/2) \\ \cos[(x+\sqrt{3}y)/4] & \cos(x/2) & 0 \end{pmatrix}, \tag{21}$$

$$\boldsymbol{J}'(\mathbf{q}) = 2J\begin{pmatrix} 2\cos(x/2)\cos(\sqrt{3}y/2) & \cos[(3x+\sqrt{3}y)/4] & \cos[(3x-\sqrt{3}y)/4] \\ \cos[(3x+\sqrt{3}y)/4] & \cos x + \cos[(x-\sqrt{3}y)/2] & \cos(\sqrt{3}y/2) \\ \cos[(3x-\sqrt{3}y)/4] & \cos(\sqrt{3}y/2) & \cos x + \cos[(x+\sqrt{3}y)/2] \end{pmatrix}. \tag{22}$$

in which $x = q_x a$ and $y = q_y a$.

It follows that

$$\boldsymbol{\chi}(\mathbf{q},\omega) = -2c_1\frac{\boldsymbol{P}(\mathbf{q},\omega^2)}{\Delta(\mathbf{q},\omega^2)} \tag{23}$$

where $\Delta(\mathbf{q},\xi)$ is a third degree polynomial in ξ with $\mathbf{q}$-dependent coefficients and the elements of $\boldsymbol{P}(\mathbf{q},\xi)$ are second degree polynomials in ξ with $\mathbf{q}$-dependent coeficients. The dynamic susceptibility can be finally writen as

$$\boldsymbol{\chi}(\mathbf{q},\omega) = -2c_1\sum_{l=1}^{3}\frac{\boldsymbol{R}_l(\mathbf{q})}{\omega^2-\Omega_l^2(\mathbf{q})} \tag{24}$$

where

$$\boldsymbol{R}_l(\mathbf{q}) = \frac{\boldsymbol{P}(\mathbf{q},\Omega_l^2)}{\Delta'(\mathbf{q},\Omega_l^2)} \tag{25}$$

and

$$\Delta'(\mathbf{q},\xi) = \frac{\partial}{\partial\xi}\Delta(\mathbf{q},\xi)\;. \tag{26}$$

The $\Omega_l(\mathbf{q})$ are excitation energies, obtained from the roots $\xi_l = \Omega_l^2(\mathbf{q})$ of the polynomial $\Delta(\mathbf{q},\xi)$. One of these roots, $\Omega_1^2(\mathbf{q}) = 6J^2(\tilde{c}+\tilde{c_1})$, is found to be non-dispersive over the whole Brillouin zone. Thus, the dispersion in the energy spectrum is due to the other roots ($l = 2, 3$), which are evaluated numerically.

By writing the correlation functions of eq. 12 in matrix form and performing the inverse Fourier transformation, we can show that

$$c^{ab}_{ij} = -2c_1\sum_{l=1}^{3}\sum_{\mathbf{q}} b_l(\mathbf{q})\; R^{ab}_l(\mathbf{q})\;\cos\{\mathbf{q}\cdot(\mathbf{R}^a_i-\mathbf{R}^b_j)\} \tag{27}$$

where

$$b_l(\mathbf{q}) = \frac{n(\Omega_l)-n(-\Omega_l)}{2\Omega_l}, \tag{28}$$

and $n(\omega)$ is the Bose distribution function. The sum over momenta must be performed numerically.

The dynamic structure factor matrix is related to the dynamic susceptibility by

$$\boldsymbol{S}(\mathbf{q},\omega) = -\frac{2\mathrm{Im}\;\boldsymbol{\chi}(\mathbf{q},\omega)}{1-e^{-\beta\omega}}. \tag{29}$$

After obtaining the selfconsistent parameters, the static

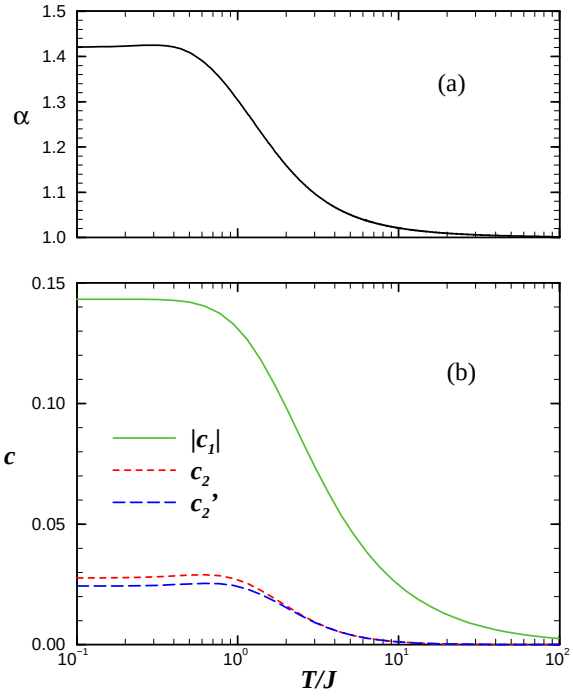

FIG. 2: (a) The selfconsistent parameter α and (b) the correlation functions c_1, c_2 and c_2' as a function of temperature.

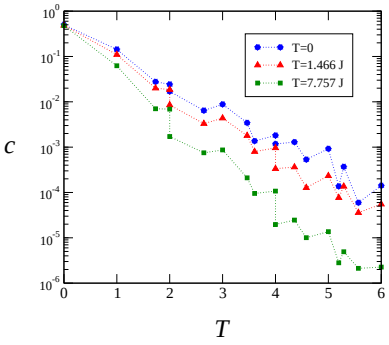

FIG. 3: Correlation functions versus distance (in units of the lattice parameter a).

structure factor can be evaluated by

$$\boldsymbol{S}(\mathbf{q}) = 2c_1 \sum_{l=1}^{3} \sum_{\mathbf{q}} b_l(\mathbf{q})\ \boldsymbol{R}_l(\mathbf{q}). \tag{30}$$

III. RESULTS

We have calculated the selfconsistent values of c_1, c_2, and c_2' as a function of temperature. They are plotted in fig. 2-b. The selfconsistent parameter α is shown in fig. 2-a. From the knowledge of these selfconsistent functions all missing correlation functions can be evaluated. In figure 3 we show the correlation functions $c_n^{(\prime)}$ between sites separated by at most 6 lattice bonds. The distribution of the points is very similar to that obtained in Ref. 24 for the pyrochlore lattice, indicating an exponential decay with a correlation length of the order of the lattice parameter a.

The internal energy is given by $E = -6NJc_1$. The ground-state value $E = -0.859NJ$ is in good agreement with earlier calculations (see Refs. 8,22,25). In figure 4 we present the specific heat $C = dE/dT$. This curve has a single peak and is very similar to the result of high-temperature expansions[10] reproducing the high-temperature limit $C \sim T^{-2}$. In the low-temperature limit, the time involved in the numerical computation increases with decreasing temperature, because the convergence of the integral in $\mathbf{q}$ becomes slower, and in addition one needs a higher precision in order to perform the derivative involved in the evaluation of the specific heat. Nevertheless, a careful analysis of the numerical results indicates unambiguously a T^2 dependence of the specific heat which extends to very low temperatures. Therefore, there will be no second peak in the present model. The fact that the specific heat does not vanish exponentially indicates the presence of low energy states even though the low-temperature peak found in Ref. 12 is missing. Indeed, it should be emphasized that it is not sure that this peak will persist in the thermodynamic limit[26] which supports the results obtained in the present work. The change in entropy $\int_0^T \frac{C(T')}{T'} dT'$ is also shown in Fig. 4. The total change in entropy is $0.54 \ln 2$, corresponding to a ground-state entropy $0.46 \ln 2$, of the same order as found in Ref. 10.

The eigenvalues $\lambda_n(\mathbf{q})$ of the structure factor are shown in Fig. 5. The result is remarkably similar to what is found from the high-temperature expansions of Ref.[10]. Whithin the present approach one can easily follow the effect of temperature on the structure factor for all wavevectors even at very low T. We observe that its highest eigenvalue is degenerate over the whole Brillouin zone. For the pyroclore, the structure factor is a 4×4 matrix, which has one additional eigenvalue. In a perturbative expansion[24] the two highest eigenvalues are found to lie very close to each other, one of them being completely degenerate while the other one has a weakly lifted degeneracy, which is crucial to reproduce the main features of neutron scattering experiments. As a further work, it would be interesting to extend the present approach to the pyrochlore antiferromagnet.

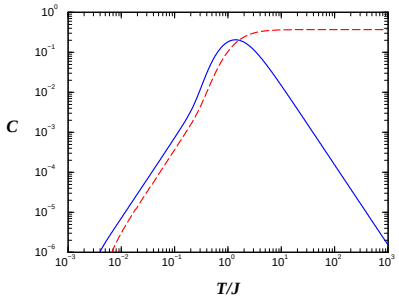

FIG. 4: Specific heat as a function of temperature (solid line). The dashed line gives the integrated entropy.

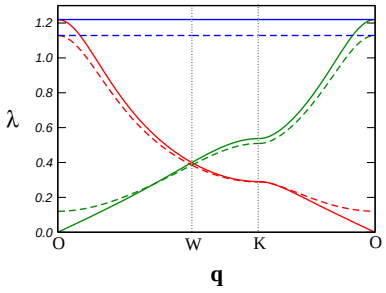

FIG. 5: The eigenvalues $\lambda_n(\mathbf{q})$ of the structure factor along some symmetry directions in $\mathbf{q}$-space at $T = 0$ (solid lines) and for an intermediate value of T (dashed lines).

Acknowledgments

This work has been partially supported by Brazilian agencies CNPq (Conselho Nacional de Desenvolvimento Científico e Tecnológico) and CAPES (Coordenação de Aperfeiçoamento de Pessoal de Nível Superior) through the French-Brazilian cooperation agreement CAPES-COFECUB.

* dfi2bhb@joinville.udesc.br
† canals@labs.polycnrs-gre.fr
‡ lacroix@labs.polycnrs-gre.fr

[1] R. Liebmann: *Statistical Mechanics of Periodic Frustrated Ising Systems*, (Springer, Berlin, 1986).
[2] A. P. Ramirez, Ann. Rev. Mater. Sci **24**, 453 (1994), P. Schiffer and A. P. Ramirez, Comments Condens. Matter Phys. **18**, 21 (1996) and references therein.

[3] P. W. Anderson, B. Halperin and C. M. Varma, Phisos. Mag. **25**, 1 (1972).
[4] V. Elser, Phys. Rev. Lett. **62**, 2405 (1989).
[5] C. Zeng and V. Elser, Phys. Rev. B **51**, 8318 (1995).
[6] J. Chalker and J. Eastmond, Phys. Rev. B **46**, 14201 (1992).
[7] P. Leung and V. Elser, Phys. Rev. B **47**, 5459 (1993).
[8] P. Lecheminant *et al.*, Phys. Rev. B **56**, 2521 (1997).
[9] C. Waldtmann *et al.*, Eur. Phys. J. B **2**, 501 (1998).
[10] N. Elstner and A. P. Young, Phys. Rev. B **50**, 6871 (1994).
[11] F. Mila, Phys. Rev. Lett. **81**, 2356 (1998).
[12] P. Sindzingre, G. Misguich, C. Lhuillier, B. Bernu, L. Pierre, Ch. Waldtmann, and H.-U. Everts, Phys. Rev. Lett. **84**, 2953 (2000).
[13] J. N. Reimers, A. J. Berlinsky and A.-C. Shi., Phys. Rev. B **43** (1991) 865.
[14] E. F. Shender, V. B. Cherepanov, P. C. W. Holdsworth, and A. J. Berlinsky, Phys. Rev. Lett. **70**, 3812-3815 (1993).
[15] M. Elhajal, B. Canals, C. Lacroix, *to be published*.
[16] A. Ramirez *et al.*, Phys. Rev. Lett. **64**, 2070 (1992).
[17] Y. Uemura *et al.*, Phys. Rev. Lett. **73**, 3306 (1994).
[18] S.-H. Lee *et al.*, Europhys. Lett **35**, 127 (1996).
[19] N. Wada *et al.*, J. Phys. Soc. Jpn. **66**, 961 (1997).
[20] J. Kondo and K. Yamaji, Prog. Theor. Phys. **47**, 807 (1972).
[21] H. Shimahara, S. Takada, J. Phys. Soc. Jap. **60**, 2394 (1991).
[22] W. Yu and S. Feng, Eur. Phys. J. B **13**, 265 (2000).
[23] M. E. Gouvêa and A. S. T. Pires, *to be published*
[24] B. Canals and C. Lacroix, Phys. Rev. Lett. **80**, 2933 (1998).
[25] Chen Zeng and Veit Elser, Phys. Rev. B **42**, 8436 (1990).
[26] P. Sindzingre, *private communication*.